



**HAL**  
open science

## Recent trends in the recurrence of North-Atlantic Atmospheric Circulation Patterns

Pascal Yiou, Julien Cattiaux, Aurélien Ribes, Robert Vautard, Mathieu Vrac

► **To cite this version:**

Pascal Yiou, Julien Cattiaux, Aurélien Ribes, Robert Vautard, Mathieu Vrac. Recent trends in the recurrence of North-Atlantic Atmospheric Circulation Patterns. 2017. hal-01616483

**HAL Id: hal-01616483**

**<https://hal.science/hal-01616483v1>**

Preprint submitted on 13 Oct 2017

**HAL** is a multi-disciplinary open access archive for the deposit and dissemination of scientific research documents, whether they are published or not. The documents may come from teaching and research institutions in France or abroad, or from public or private research centers.

L'archive ouverte pluridisciplinaire **HAL**, est destinée au dépôt et à la diffusion de documents scientifiques de niveau recherche, publiés ou non, émanant des établissements d'enseignement et de recherche français ou étrangers, des laboratoires publics ou privés.

# 1 Recent trends in the recurrence of North- 2 Atlantic Atmospheric Circulation Patterns

---

3 P. Yiou (1), J. Cattiaux (2), A. Ribes (2), R. Vautard (1), M. Vrac (1)

4 (1) Laboratoire des Sciences du Climat et de l'Environnement, UMR CEA-CNRS-UVSQ,  
5 IPSL & U Paris-Saclay, CE l'Orme des Merisiers, 91191 Gif-sur-Yvette

6 (2) Centre National de Recherches Météorologiques, UMR CNRS - Météo-France, 42 avenue  
7 G. Coriolis 31057 Toulouse, France

8

## 9 **Abstract**

10 A few types of extreme climate events in the North Atlantic region, such as heatwaves, cold  
11 spells or high cumulated precipitation, are connected to the persistence of atmospheric  
12 circulation patterns. Understanding or attributing those extreme events requires assessing  
13 long-term trends of the atmospheric circulation. This paper presents a set of diagnostics of the  
14 intra and interannual recurrence of atmospheric patterns. Those diagnostics are devised to  
15 detect trends in the stability of the circulation and the return period of atmospheric patterns.  
16 We detect significant emerging trends in the winter circulation, pointing towards a potential  
17 increased predictability. No such signal seems to emerge in the summer. We find that the  
18 winter trends in the dominating atmospheric patterns and their recurrences do not depend of  
19 the patterns themselves.

## 20 **Introduction**

21 Recent North Atlantic winter and summer extremes have been associated with persistent  
22 patterns of atmospheric circulation. Those patterns have been rather contrasted from one year  
23 to another. Cold spells of January 2010, December 2010 and February 2012 in Europe  
24 resulted from persisting blocking situations over Scandinavia [*Cattiaux et al.*, 2010; *Cohen et*  
25 *al.*, 2010]. Warm winter 2006/2007 [*Cattiaux et al.*, 2009; *Yiou et al.*, 2007] and stormy  
26 winter 2013/14 [*Huntingford et al.*, 2014; *van Oldenborgh et al.*, 2015] were dominated by  
27 persistent high-pressure systems over the Azores and the Mediterranean sea, respectively. The

28 low-wind month of December 2016 was dominated by a persisting high pressure center over  
29 North-Western Europe [Vautard *et al.*, 2017]. The warm summers of 2003 and 2015 in  
30 Europe were associated with either a persisting blocking pattern over Scandinavia or Atlantic  
31 low conveying warm air into Europe from North Africa. Therefore it is difficult to claim that  
32 a given atmospheric pattern has dominated during recent years to create such climate  
33 extremes. However it has been speculated that the amplitude of atmospheric patterns is  
34 changing, in particular through a connection between Arctic sea-ice cover and meanders of  
35 the jet stream [Francis and Vavrus, 2012; Petoukhov *et al.*, 2013]. The statistical significance  
36 of such a trend as well as the relevance of the evoked mechanisms has been debated [Barnes,  
37 2013; Screen and Simmonds, 2013a; b].

38 The mid-latitude atmospheric variability is characterized by a baroclinic instability of the  
39 zonal flow [Hoskins and James, 2014]. This instability grows into Rossby waves. It has been  
40 argued that the excitation conditions those Rossby waves have increased in the past decades  
41 [Petoukhov *et al.*, 2013; Petoukhov *et al.*, 2016].

42 [Faranda *et al.*, 2016] studied how unstable fixed points of the extra-tropical atmospheric  
43 circulation correspond to blocking patterns. [Faranda *et al.*, 2017] investigated the local  
44 dimension of North Atlantic atmospheric circulation, and examined the implications for  
45 predictability in the winter season.

46 In this paper, we analyze recently observed trends in the surface North Atlantic circulation in  
47 winter and summer. We examine trends in the intra-seasonal recurrence of flow patterns by  
48 introducing the notion of recurrence “networks” within a season. The interannual pattern trend  
49 is examined by the probability of detecting good analogues of circulation. Those intra and  
50 inter annual diagnostics allow to detect emerging properties of the atmospheric circulation.

## 51 **Data and Methods**

52 We use the reanalysis data of the National Centers for Environmental Prediction (NCEP)  
53 [Kistler *et al.*, 2001] between January 1948 and March 2017. We consider the sea-level  
54 pressure (SLP) over the North Atlantic (80W-30E; 30-70N). One of the caveats of this  
55 reanalysis dataset is the lack of homogeneity of assimilated data, in particular before the  
56 satellite era. This can lead to breaks in pressure related variables, although such breaks are  
57 mostly detected in the southern hemisphere and the Arctic regions [Sturaro, 2003].

58 The first concept we develop is the intra-seasonal recurrence of atmospheric patterns for the  
59 winter and summer seasons (December-January-February (DJF) and June-July-August (JJA)).

60 The temporal autocorrelation (number of days with an autocorrelation significantly above 0)  
61 of SLP around the North Atlantic is close to 5 days on average [Yiou *et al.*, 2012]. If the  
62 atmospheric circulation fluctuates around a given state on time scales that are longer than 5  
63 days, this might not be reflected by the sample autocorrelation. Beyond the formal  
64 persistence, we are interested in the fact that the atmosphere could come back to a given  
65 pattern, after a significant disturbance. This identifies a recurrent --- although unstable ---  
66 state of the atmosphere, potentially corresponding to a wave excitation. We adopt two ways  
67 of measuring the intra-seasonal recurrence of patterns within a season.

68 The first one is based on the analysis of weather regimes of the atmospheric circulation. For  
69 each season, the SLP anomalies (with respect to the seasonal cycle) are classified onto four  
70 weather regimes. The daily seasonal cycle is computed with a smoothing spline of daily  
71 averages. We compute the principal components (PCs, [von Storch and Zwiers, 2001]) of the  
72 NCEP reanalysis SLP data. The weather regimes (WR) are determined by a *k*-means  
73 clustering of the first 10 PCs, between 1970 and 2000 [Michelangeli *et al.*, 1995; Yiou *et al.*,  
74 2008]. The WR patterns depend on the season, as well as their effects on surface variables  
75 such as precipitation and temperature. For each year and each season (winter and summer),  
76 the daily SLP patterns are attributed to the closest WR pattern (in terms of Euclidean  
77 distance). The annual frequency of WR is the ratio of the occurrence of the WR to the length  
78 of the season. For each year and each season, the *dominant* WR is the one with the highest  
79 frequency, and we report the frequency of the dominant weather regime.

80 The second approach to that concept is based on the similarity of intra-seasonal daily SLP  
81 patterns. For each reference day within a season, we determine all the days of the same season  
82 that yield a spatial rank correlation that exceeds a threshold  $r$ . Here, we take  $r = 0.5$ , which  
83 corresponds to the 60<sup>th</sup> percentile of all intra-seasonal sample correlation values. Hence, we  
84 construct a “network” of resembling days, for each season. The dominating network is the one  
85 that yields the largest number of similar patterns. This approach is akin to the dominating WR  
86 analysis, but it does not constrain the geographical location of the recurrent weather pattern.

87 The fluctuations of the frequencies of the dominating WR or the “network” sizes help us  
88 assess how the persistence of atmospheric patterns varies through time. Those two intra-  
89 seasonal quantities (frequency of dominating weather regime and size of dominating network)  
90 allow investigating recurrent but potentially unstable patterns of the atmospheric circulation.  
91 Those patterns do not need to be visited in spates of consecutive days. Those two approaches  
92 are meant to determine the trend of intra-seasonal pattern recurrence. This concept is distinct  
93 from the clustering index examined by [Faranda *et al.*, 2017], which focuses on the local

94 persistence of the system. But the concept is complementary to the analyses of [Faranda et  
95 al., 2016] because we identify unstable fixed points (in the phase space of the atmospheric  
96 circulation) to which trajectories “try” to come back close to.

97 The second concept is the interannual recurrence of SLP patterns. The emergence (or  
98 disappearance) of patterns is estimated from interannual analogues of circulation [Yiou et al.,  
99 2007]. For each day, we determine the best 20 analogues of circulation by minimizing a  
100 distance to all days occurring in a different year, but at most 30 calendar days apart. Good  
101 analogues have a distance that is smaller than a threshold  $d_0$  corresponding to the 25<sup>th</sup>  
102 percentile of distance, and a spatial correlation that is higher than a threshold  $r_0 = 0.5$   
103 corresponding to the 75<sup>th</sup> percentile of spatial correlations of all 20 best analogues. In practice,  
104 the number of good analogues for a given day is always lower than 10 for such data.  
105 Therefore retaining more than the 20 best analogues would not change the results. The  
106 distributions of correlations for interannual analogues (i.e. picked in another year) and intra-  
107 seasonal analogues are different, which explains that the value  $r = 0.5$  corresponds to  
108 different quantiles in the two cases. The seasonal average number of good analogues is a  
109 proxy for the probability of observing a circulation pattern and gives access to the usual  
110 character of a season. If this number decreases, then one can conclude that the circulation  
111 during that season becomes less typical, leading to the appearance of new patterns with no  
112 past analogues.

## 113 Results

114 The frequency of the dominating analogue pattern yields a positive trend in winter (1% of  
115 winter days per decade, p-value=0.045) (Figure 1, dashed black lines), and a negative trend in  
116 summer (-1% of summer days per decade, p-value= $8 \cdot 10^{-4}$ ) (Figure 2, dashed black lines). The  
117 positive winter trend is unstable, due to the upward fluctuation in the 1990s: the trend since  
118 1980 (the use of satellite data in the reanalysis) is close to 0 and not significant, and the trend  
119 since 1997 (with the optimal number of assimilated observations) is 1.3% per decade. The  
120 summer trend over 1950-2017 is also unstable, with negligible and insignificant trends since  
121 1980 and 1997. The number of days spent in the summer dominating weather regimes (~38  
122 days) or the preferred state (~20 days) is smaller than in the winter (resp. 40 days and 30  
123 days). From a count of the dominant WR frequencies in Figure 1, the zonal weather regime  
124 (ZO) has been preferred in the winter between 1948 and 2015. The ZO weather regime  
125 dominated 35% of winters (BLO: 29%; NAO- : 19%; AR: 16%). Those weather regimes have

126 dominated winters roughly equi-probably since 2000. The preferred summer weather regime  
127 (Figure 2) has been the Scandinavian blocking (BLO: 40% of summers) (against NAO-: 21%;  
128 AR: 21%; AT: 18%). The summer Atlantic Ridge (AR) has dominated only once since 2000  
129 and the other three weather regimes have been rather equi-probable. The AR weather regime  
130 is unlikely during warm summers [Cassou *et al.*, 2005]. The period since 2000 has been the  
131 longest spell with so few AR occurrences since 1948, although it is difficult to interpret the  
132 behavior of the last 15 years in terms of an emerging signal, because of the large decadal  
133 variability of the dominating regimes. A similar analysis of the 20CR reanalysis ensemble  
134 mean [Compo *et al.*, 2011] provides the same results on the 1948—2012 period (not shown).  
135 The period before 1948 does not yield any significant trend, but this could be due to the large  
136 ensemble spread whose averaging smears out trends (not shown).

137 We identify five winters with the largest number of similar days (1969, 1989, 1990, 2010 and  
138 2014). The SLP patterns for those years are shown in Figure 3. The winters that are identified  
139 yield zonal (1989, 1990 and 2014) or NAO- (1969 and 2010) weather regimes. We also find  
140 that the winters between 1948 and 2014 with more than 35 similar days are in one of those  
141 two weather regimes. The extremely persistent winter patterns are the two phases of the North  
142 Atlantic Oscillation, that generate either stormy and warm surface conditions (ZO regime), or  
143 wet and cold conditions (NAO- regime) over Western Europe.

144 The five summers for which the recurrence is highest (larger than 25%) are mostly in the  
145 Atlantic Ridge regime (4 occurrences) and Scandinavian Blocking (1 occurrence) (Figure 2).  
146 By contrast, the five most frequent summer weather regimes (more than 45%) are the  
147 Scandinavian Blocking (3 occurrences), Atlantic Ridge (1 occurrence) and Atlantic Low (1  
148 occurrence). This shows that the maximum occurrence of a weather regime within a season is  
149 disconnected from its interannual frequency: the summer AR regime is the most recurrent but  
150 is not very frequent. Such high recurrence values do not occur after 2000.

151 The average number of good circulation analogues characterizes the recurrence of the patterns  
152 in time. Hence, seasons with few good analogues can be considered as rare, while those with  
153 many good analogues are typical. A trend in the number of good analogues indicates a shift in  
154 the atmospheric circulation pattern, which might not be detectable in the frequency of weather  
155 regimes. Figure 4 shows the time variations of the mean number of good intra-seasonal  
156 analogues for the summer and winter. The winter series yields a small but significant positive  
157 trend (0.1 analogue day per decade,  $p\text{-value}=8 \cdot 10^{-3}$ , Figure 4a). This means that the daily  
158 circulation patterns tend to become more clustered during the last decades, because the  
159 circulation analogues become increasingly good.

160 The summer series yields a significant negative trend (-0.07 analogue day per decade, p-  
161 value= $8 \cdot 10^{-3}$ , Figure 4b). This means that the daily patterns have become individually more  
162 exceptional, although not necessarily extreme, from the first part of the period to the second  
163 part. The latter JJA decreasing trend does not hold for the last two decades (1990—2016),  
164 which yield a slightly positive trend. Therefore, this trend can hardly be interpreted in terms  
165 of a climate change signal, because it is likely to be influenced by decadal internal variability.

## 166 Discussion

167 The increasing trend of similar atmospheric patterns in winter started only recently, in the  
168 1970s (Figure 1). This trend means that the patterns become more clustered at the intra-  
169 seasonal scale, with a locking to the phases of the North Atlantic Oscillation. Trends in the  
170 frequencies of those two weather regimes either bring prolonged episodes of snowfall to  
171 Europe (like in 2010, with an NAO- phase), or prolonged stormy episodes and precipitation  
172 episodes over northern Europe (like in 2014, with zonal circulation). The concomitant  
173 increasing trend of the probability of finding a good winter circulation analogue (Figure 4a)  
174 suggests that the return periods of observed winters become shorter, so that winters tend to be  
175 similar to already known winters.

176 The decreasing trend of similar weather patterns in the summer means that slow building  
177 extreme events, such as droughts and heatwaves or cold summers, tend to be less frequent in  
178 Europe. The concomitant decreasing trend of interannual pattern recurrence suggests that  
179 summers become less similar to already known ones, although this trend is very small.

180 Those results can be interpreted in terms of an increase of predictability of the circulation in  
181 the winter because the size of the dominating weather patterns increases. There would be no  
182 such trend of predictability in the summer. Therefore, a prediction based on persistence would  
183 have an increased skill in the winter.

184 Our analyses seem to contradict the hypothesis of increased winter mid-latitude atmospheric  
185 meandering described by [Francis and Vavrus, 2012; Petoukhov et al., 2013], because the  
186 winters with the most recurrent weather types we detect have had rather low wave numbers at  
187 the surface [Cattiaux et al., 2016] while they were associated to extremely warm and stormy  
188 conditions (1989, 1990, 2014) or extremely snowy conditions (1969, 2010) (Figure 3). Arctic  
189 sea-ice cover before those winters was either lower or above normal, and the meridional  
190 gradient of potential temperature did not show a systematic feature for those five cases, due to  
191 the fact that they correspond to opposite phases of the NAO. Yet, our analysis reaches similar

192 conclusions on the impacts on European surface winter climate, in that more persistent zonal  
193 flows increase the probability of observing extra-tropical storms hitting Europe or extreme  
194 precipitation amounts in Northern Europe, as in 1999/2000 and 2013/2014. Conversely,  
195 prolonged spells of negative phase of the NAO in the winter increases the probability of  
196 extreme precipitation (including snow) in Southern Europe, as in 1969 and 2010. Our  
197 interpretation is that the atmospheric patterns that dominate during the winter tend to get  
198 “trapped” for longer times, although they are not necessarily more stable. We propose a  
199 conceptual model for this behavior, with an energy potential model in two dimensions with  
200 four wells whose relative depth varies randomly from one year to the next. Daily  
201 perturbations can force the system to shift wells, but at the end of the season, the deepest well  
202 is the most visited. We find that the deepest well becomes deeper in the winter.  
203 The same analyses (persistence of SLP patterns) were performed for the North Pacific region  
204 and the whole Northern hemisphere extra-tropics (not shown). No trend is found on such  
205 regions and scales.

## 206 **Conclusion**

207 In this paper, we have shown significant, albeit small, emerging trends of recurrence  
208 properties of the atmosphere over the North Atlantic. Those trends point to increased  
209 atmospheric predictability in winter. This is coherent with the small decrease of local  
210 dimension reported by [Faranda *et al.*, 2017]. The diagnostics we proposed have an  
211 interesting potential to assess the atmospheric temporal variability of climate models,  
212 especially for paleoclimates or future scenarios [Schmidt *et al.*, 2014]. Our results can be used  
213 to estimate a dynamical contribution in the attribution of extreme events [National Academies  
214 of Sciences and Medicine, 2016; Shepherd, 2016; Yiou *et al.*, 2017], which is considered as a  
215 small signal to identify [Shepherd, 2016; Yiou *et al.*, 2017]. We have not determined the cause  
216 of the winter circulation trends, which could be tied to internal variability [Cattiaux *et al.*,  
217 2016], but this observed emerging trend has an effect on the event attribution process.

## 218 **Acknowledgements**

219 It is a pleasure to thank C. Cassou for discussions at an early stage of this research. This paper  
220 was supported by ERC Grant No. 338965-A2C2 and French Ministry of Environment Grant  
221 “Extremoscope”.



## 222 **Conflict of interest**

223 The author declare that there is no conflict of interest regarding the publication of this paper.

## 224 **Author contributions**

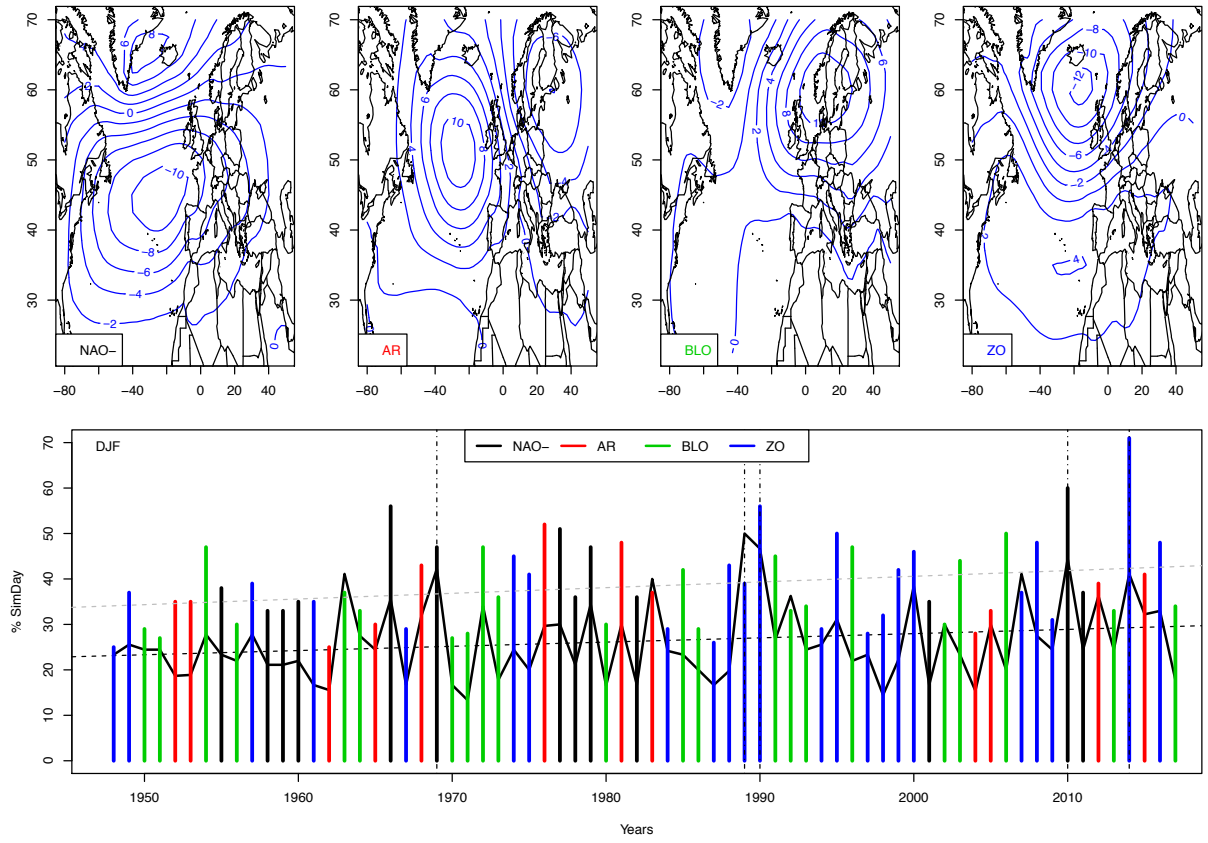
225 PY and RV designed the analysis on analogue “networks”. PY produced the figures and draft  
226 manuscript. All co-authors contributed to the manuscript and figure design.

## 227 **References**

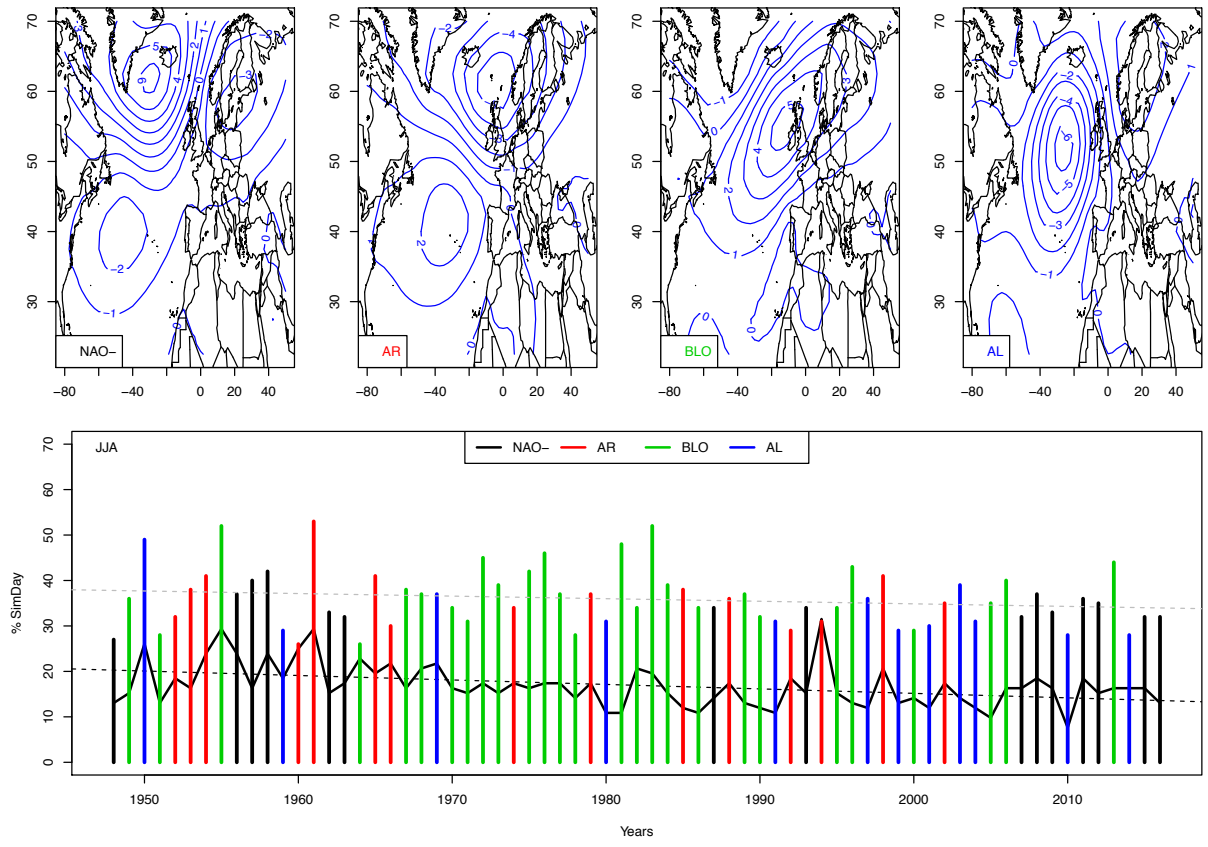
- 228 Barnes, E. A. (2013), Revisiting the evidence linking Arctic amplification to extreme weather  
229 in midlatitudes, *Geophys. Res. Lett.*, *40*(17), 4734-4739.
- 230 Cassou, C., et al. (2005), Tropical Atlantic influence on European heat waves, *J. Clim.*,  
231 *18*(15), 2805-2811.
- 232 Cattiaux, J., et al. (2009), Origins of the extremely warm European fall of 2006, *Geophys.*  
233 *Res. Lett.*, *36*, doi:10.1029/2009GL037339.
- 234 Cattiaux, J., et al. (2010), Winter 2010 in Europe: A cold extreme in a warming climate,  
235 *Geophys. Res. Lett.*, *37*(L20704), 10.1029/2010gl044613.
- 236 Cattiaux, J., et al. (2016), Sinuosity of midlatitude atmospheric flow in a warming world,  
237 *Geophys. Res. Lett.*, *43*(15), 8259-8268.
- 238 Cohen, J., et al. (2010), Winter 2009-2010: A case study of an extreme Arctic Oscillation  
239 event, *Geophys. Res. Lett.*, *37*(L17707).
- 240 Compo, G. P., et al. (2011), The Twentieth Century Reanalysis Project, *Quat. J. Roy. Met.*  
241 *Soc.*, *137*(654), 1-28.
- 242 Faranda, D., et al. (2016), The switching between zonal and blocked mid-latitude atmospheric  
243 circulation: a dynamical system perspective, *Clim. Dyn.*, *47*(5-6), 1587-1599.
- 244 Faranda, D., et al. (2017), Dynamical proxies of North Atlantic predictability and extremes,  
245 *Scientific Reports*, *7*(Artn 41278).
- 246 Francis, J. A., and S. J. Vavrus (2012), Evidence linking Arctic amplification to extreme  
247 weather in mid-latitudes, *Geophys. Res. Lett.*, *39*(L06801).
- 248 Hoskins, B., and I. N. James (2014), *Fluid dynamics of the midlatitude atmosphere*, xviii, 408  
249 pages pp., J. Wiley and sons, Chichester.
- 250 Huntingford, C., et al. (2014), Potential influences on the United Kingdom's floods of winter  
251 2013/14, *Nature Climate Change*, *4*(9), 769-777.

- 252 Kistler, R., et al. (2001), The NCEP-NCAR 50-year reanalysis: Monthly means CD-ROM and  
253 documentation, *Bull. Amer. Meteorol. Soc.*, 82(2), 247-267.
- 254 Michelangeli, P., et al. (1995), Weather regimes: Recurrence and quasi-stationarity, *J. Atmos.*  
255 *Sci.*, 52(8), 1237-1256.
- 256 National Academies of Sciences, E., and Medicine (2016), *Attribution of Extreme Weather*  
257 *Events in the Context of Climate Change*, 186 pp., The National Academies Press,  
258 Washington, DC.
- 259 Petoukhov, V., et al. (2013), Quasiresonant amplification of planetary waves and recent  
260 Northern Hemisphere weather extremes, *Proc. Natl. Acad. Sci. USA*, 110(14), 5336-5341.
- 261 Petoukhov, V., et al. (2016), Role of quasiresonant planetary wave dynamics in recent boreal  
262 spring-to-autumn extreme events, *Proc. Natl. Acad. Sci. USA*, 113(25), 6862-6867.
- 263 Schmidt, G. A., et al. (2014), Using palaeo-climate comparisons to constrain future  
264 projections in CMIP5, *Climate of the Past*, 10(1), 221-250.
- 265 Screen, J. A., and I. Simmonds (2013a), Caution needed when linking weather extremes to  
266 amplified planetary waves, *Proc. Natl. Acad. Sci. USA*, 110(26), E2327-E2327.
- 267 Screen, J. A., and I. Simmonds (2013b), Exploring links between Arctic amplification and  
268 mid-latitude weather, *Geophys. Res. Lett.*, 40(5), 959-964.
- 269 Shepherd, T. G. (2016), A Common Framework for Approaches to Extreme Event  
270 Attribution, *Current Climate Change Reports*, 2(1), 28-38.
- 271 Sturaro, G. (2003), A closer look at the climatological discontinuities present in the  
272 NCEP/NCAR reanalysis temperature due to the introduction of satellite data, *Clim. Dyn.*,  
273 21(3-4), 309--316.
- 274 van Oldenborgh, G. J., et al. (2015), Drivers of the 2013/14 winter floods in the UK, *Nature*  
275 *Clim. Change*, 5, 490-491.
- 276 Vautard, R., et al. (2017), Attribution of wintertime anticyclonic stagnation contributing to air  
277 pollution in Western Europe, *Bull. Amer. Meteorol. Soc.*, subjudice.
- 278 von Storch, H., and F. W. Zwiers (2001), *Statistical Analysis in Climate Research*, Cambridge  
279 University Press, Cambridge.
- 280 Yiou, P., et al. (2007), Inconsistency between atmospheric dynamics and temperatures during  
281 the exceptional 2006/2007 fall/winter and recent warming in Europe, *Geophys. Res. Lett.*,  
282 34(L21808), doi:10.1029/2007GL031981.
- 283 Yiou, P., et al. (2008), Weather regime dependence of extreme value statistics for summer  
284 temperature and precipitation, *Nonlin. Proc. Geophys.*, 15, 365–378.
- 285 Yiou, P., et al. (2012), Ensemble reconstruction of the atmospheric column from surface  
286 pressure using analogues, *Clim. Dyn.*, 41(5-6), 1333-1344.

287 Yiou, P., et al. (2017), A statistical framework for conditional extreme event attribution, *Adv.*  
 288 *Stat. Clim. Meteorol. Oceanogr.*, 3(1), 17--31.  
 289  
 290  
 291  
 292  
 293



294  
 295 **Figure 1: Upper panels: four weather regimes of SLP anomalies in DJF (negative phase of the NAO, Atlantic Ridge,**  
 296 **Scandinavian Blocking, zonal flow). The isolines have increments of 2 hPa. Lower panel: Trends in atmospheric**  
 297 **persistence for DJF. Vertical colored lines: frequency of dominating weather regime. The color is associated with a**  
 298 **weather regime (NAO-: black; AR: red; BLO: green; ZO: blue). Gray dotted lines are for the linear trend of regime**  
 299 **frequencies. Continuous black line: maximum percentage of similar days in the winter. Dashed black lines are for the**  
 300 **linear trend of similar days. Vertical dash-dotted lines are for the five years with the largest numbers of similar days**  
 301 **(1969, 1989, 1990, 2010 and 2014).**

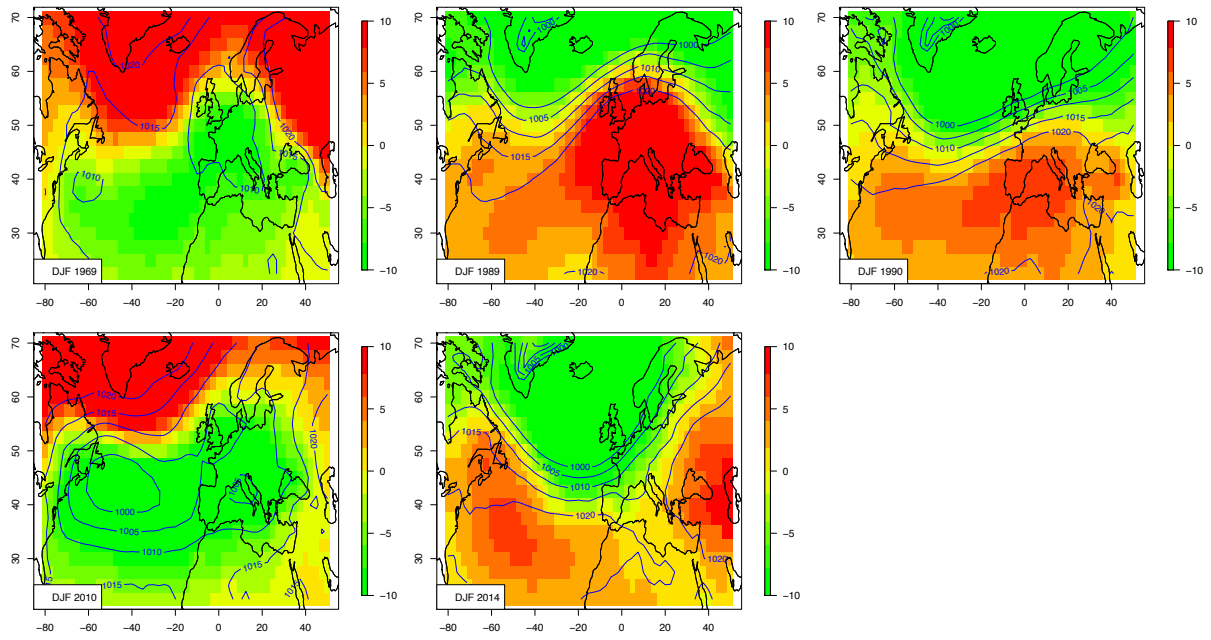


302

303 **Figure 2:** Upper panels: four weather regimes of SLP in JJA (negative phase of the NAO, Atlantic Ridge,  
 304 Scandinavian Blocking, Atlantic Low). The isolines have increments of 2 hPa. Lower panel: Trends in atmospheric  
 305 persistence for JJA. Vertical colored lines: frequency of dominating weather regime. The color is associated with a  
 306 weather regime (NAO-: black; AR: red; BLO: green; AT: blue). Gray dotted lines are for the linear trend of regime  
 307 frequencies. Continuous black line: maximum percentage of similar days in the winter. Dashed black lines are for the  
 308 linear trend of similar days.

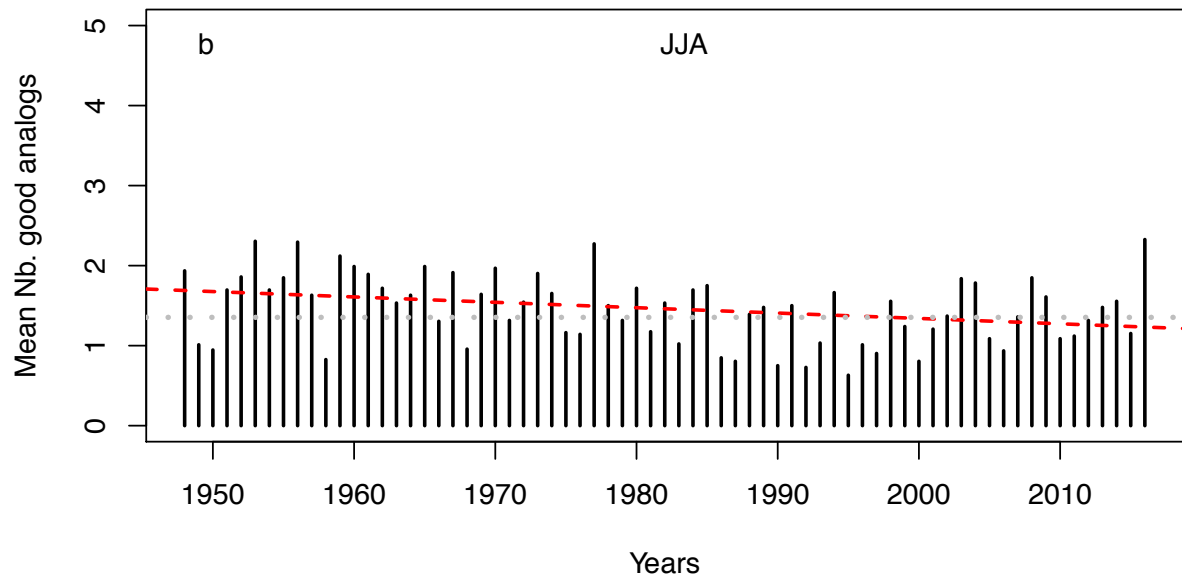
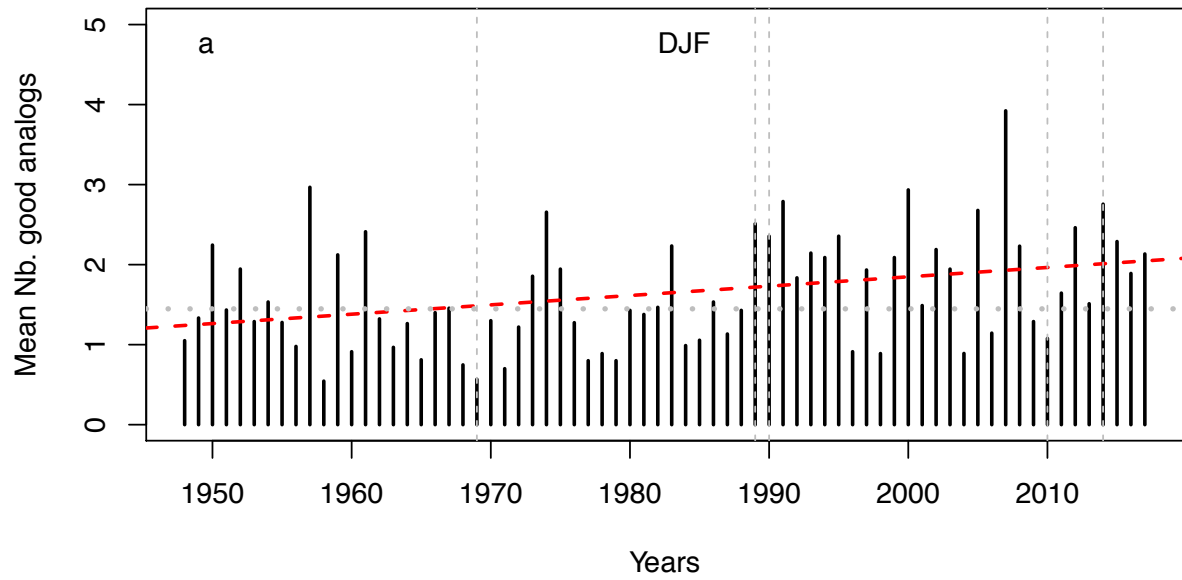
309

310



311

312 **Figure 3: Composite of SLP for the clusters of similar winter days for the five years outlined in the text (1969, 1989,**  
 313 **1990, 2010 and 2014). The isolines represent the SLP with increments of 5hPa. The colors represent anomalies of SLP**  
 314 **(in hPa) with respect to a mean seasonal cycle computed at each gridcell.**



315  
 316 **Figure 4: Average daily number of good analogues for the winter (DJF: panel a) and summer (JJA: panel b). The**  
 317 **horizontal dotted lines indicate the mean value for all years. The red dashed line is the linear regression of the number**  
 318 **of good analogues with time. The vertical dashed lines for panel a indicate the five reference winters (1969, 1989, 1990,**  
 319 **2010 and 2014).**

320  
 321  
 322